

equatorial plane is equivalent to an absorbing plane. For this reason, we form the limit function

$$\nu(r, \theta, \varphi; \tau) = \lim_{\epsilon \rightarrow 0} \lim_{\gamma \rightarrow 0} \epsilon^{-1} n(r, \theta, \varphi; \tau) = \left( \frac{2}{\pi^3 R^7} \right)^{1/2} \cos \theta \sum_{i=1}^{\infty} \left( \frac{s_i^3}{r} \right)^{1/2} \frac{J_{3/2}(s_i r/R)}{[J_{3/2}'(s_i)]^2} e^{-s_i^2 \tau/R^2} \quad (\text{B4})$$

In the limit  $\epsilon \rightarrow 0$  in eq B3, only the terms with  $n = 1$  survive. The sum on  $\alpha$  is replaced by an equivalent sum on  $i$  where  $s_i$  denotes the  $i$ th positive root of  $J_{3/2}(x) = 0$ . The limit function  $\nu(r, \theta, \varphi; \tau)$  is proportional to the probability density of the location of the chain end at  $r, \theta, \varphi$  (in the hemisphere of radius  $R$  above the impenetrable equatorial plane) for those chains of length  $\tau$  which start immediately above the origin and never wander outside the hemisphere of radius  $R$ . The integral over the hemisphere,

$$\psi(R, \tau) = \int_0^R dr \int_0^{\pi/2} d\theta \sin \theta \int_0^{2\pi} d\varphi / \nu(r, \theta, \varphi; \tau) = \frac{1}{R} \sum_{i=1}^{\infty} \left( \frac{2}{\sin^2 s_i} - \frac{2}{s_i \sin s_i} - \frac{s_i}{\sin s_i} \right) e^{-s_i^2 \tau/R^2} \quad (\text{B5})$$

is proportional to the fraction of all chains which start at

the origin, are of length  $\tau$ , and are contained in the hemisphere of radius  $R$  above an impenetrable surface. The normalized fraction is

$$\Psi(R, \tau) = c^{-1} \psi(R, \tau)$$

where

$$c = \lim_{R \rightarrow \infty} \psi(R, \tau)$$

## References and Notes

- (1) M. V. Volkenstein, "Configuration Statistics of Polymeric Chains", Interscience, New York, N.Y., 1963, Chapter 4.
- (2) H. Yamakawa, "Modern Theory of Polymer Solutions", Harper and Row, New York, N.Y., 1971, Chapter 2.
- (3) A. Katchalsky, O. Kuenzle, and W. Kuhn, *J. Polym. Sci.*, **5**, 283 (1950).
- (4) E. A. DiMarzio and R. J. Rubin, *J. Chem. Phys.*, **55**, 4318 (1971).
- (5) C. A. Hollingsworth, *J. Chem. Phys.*, **16**, 544 (1948).
- (6) M. J. Lighthill, "Fourier Analysis and Generalized Functions", Cambridge University Press, New York, N.Y., 1958, pp 67–71.
- (7) The explicit result in eq 10 was obtained independently by J. J. Weidmann, H. Kuhn, and W. Kuhn, *J. Chim. Phys. Phys.-Chim. Biol.*, **50**, 226 (1953).
- (8) The results reported here were announced in R. J. Rubin and G. H. Weiss, *Bull. Am. Phys. Soc.*, **21**, 374 (1976).
- (9) P. M. Morse and M. Feshbach, "Methods of Theoretical Physics", Vol. 1, McGraw-Hill, New York, N.Y., 1953, p 489.
- (10) H. S. Carslaw and J. C. Jaeger, "Conduction of Heat in Solids", 2nd ed, Oxford University Press, London, 1959, p 250.

# Notes

## Entanglement Networks of 1,2-Polybutadiene Cross-Linked in States of Strain. 6. The Second State of Ease

HSIN-CHIA KAN and JOHN D. FERRY\*

Department of Chemistry, University of Wisconsin, Madison, Wisconsin 53706. Received May 30, 1978

The cross-linking of 1,2-polybutadiene strained in simple extension has been described in previous papers of this series.<sup>1–3</sup> When a strained sample with stretch ratio  $\lambda_0$  is cross-linked with  $\gamma$  irradiation near the glass transition temperature ( $T_g$ ), the resulting cross-link network traps the entanglements originally present; after release and warming, the sample seeks a state of ease with stretch ratio  $\lambda_s$  in which the forces associated with the cross-links and the trapped entanglements act in opposite directions. From  $\lambda_0$  and  $\lambda_s$ , together with stress-strain measurements in small extensions from the state of ease, or simply from the equilibrium stress at  $\lambda_0$ , the concentration of trapped entanglement strands  $\nu_N$  can be calculated; the proportion of entanglements trapped,  $T_e$ , can be compared<sup>3</sup> with the theory of Langley.<sup>4</sup>

It was recognized when these experiments were undertaken<sup>5,6</sup> that untrapped entanglements might at first contribute to the retractive force toward the original unstrained state so that a first state of ease  $\lambda_s'$  would be reached followed by partial reversal of the retraction to a second state of ease  $\lambda_s$  as the strands terminated by untrapped entanglements rearrange their configurations. Until recently, only one state of ease was observed; ordinarily, the retraction kinetics and the relaxation of untrapped entanglement strands involve similar time scales and are not distinguishable.<sup>3</sup> However, if the degree of cross-linking is very slight, and precise length measure-

ments are made, a reversal of retraction can be observed, as described in the present note.

A 1,2-polybutadiene with 96% vinyl microstructure, number-average molecular weight 96 000,  $T_g$   $-10^\circ\text{C}$ , generously supplied by Dr. G. G. A. Böhm of Firestone Tire and Rubber Company (previously<sup>3</sup> identified as Polymer C), was strained in simple extension to a stretch ratio  $\lambda_0$  of approximately 1.9 and cross-linked by  $\gamma$  irradiation as previously described.<sup>1–3</sup> Distances between fiducial marks on the sample strip were measured by a travelling microscope before irradiation. During irradiation, the sample was attached to a steel band,<sup>3</sup> and after irradiation the stretched length was measured on the band. Finally, the sample was released and flattened on a base of Teflon; distances were measured again by a travelling microscope, first at  $0^\circ\text{C}$ , then at higher temperatures where the relaxation processes are faster. All lengths were corrected for thermal expansion with a linear expansion coefficient of  $2.5 \times 10^{-4} \text{ deg}^{-1}$  to a reference temperature of  $23^\circ\text{C}$ . Only the last portion of the retraction is measured by this procedure, since 80% of it or more occurs before the first measurements are taken.

From the values of  $\lambda_0$  and  $\lambda_s$ , the ratio  $R_0' = \nu_x/\nu_N$  can be calculated, where  $\nu_x$  is the concentration of network strands terminated by cross-links, by use of a three-constant Mooney–Rivlin formulation.<sup>2</sup> With additional data on stress-strain relations in deformation from the state of ease, both  $\nu_x$  and  $\nu_N$  can be calculated, and from them the average number of cross-link points per original molecule ( $\gamma$ ) and the experimental fraction of entanglements trapped ( $T_e$ ). For one sample, these quantities were estimated from other data on a sample with similar thermal history and irradiation dose. All values are summarized in Table I for these experiments.

Table I

expt no.	dose, eV/g $\times 10^{-20}$	$\lambda_0$	$\lambda_s$	$R_0'$	$\nu_N$ , mol/cm <sup>3</sup> $\times 10^4$	$\nu_x$ , mol/cm <sup>3</sup> $\times 10^4$	$\gamma$	$T_e$
239	1.5	1.968	1.128	0.255	0.48 <sup>a</sup>	0.12 <sup>a</sup>	2.3 <sup>a</sup>	0.20 <sup>a</sup>
243	3.0	1.867	1.179	0.418	1.39	0.58	7.3	0.56
245	4.5	1.850	1.222	0.561	1.83	1.03	12.1	0.74

<sup>a</sup> Estimated from data on a sample with similar dose and thermal history.

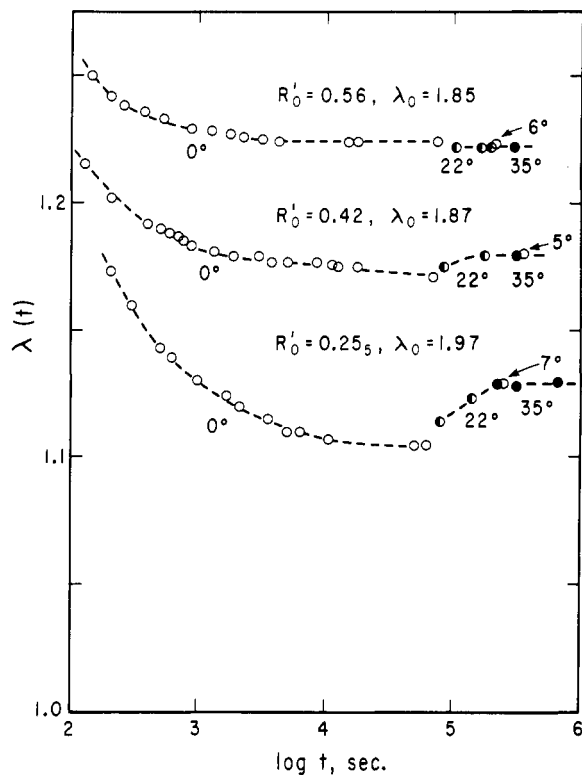


Figure 1. Retraction to the state of ease: plots of  $\lambda(t)$  against  $\log t$  for three samples at temperatures indicated (corrected for thermal expansion). Additional information is given in Table I.

The stretch ratio during retraction,  $\lambda(t)$ , is plotted against the logarithm of time  $t$  after release in Figure 1. The temperatures at which measurements were made are indicated. For the lowest cross-linking,  $R_0' = 0.255$ , a reversal is seen after the sample is warmed to increase the molecular mobility. If the temperature had been kept at 0 °C, a far longer time would have been required. After the final state of ease is reached, there is no effect of temperature, as shown by alternation of low and high temperatures. For higher cross-linking,  $R_0' = 0.42$ , the reverse retraction is much less, and for  $R_0' = 0.56$  it is absent.

The slow reversal can be attributed to the relaxation of untrapped entanglements on dangling branched structures, as can the very slow relaxation processes observed in conventional networks with low degrees of cross-linking.<sup>7,8</sup> Recent statistical calculations by Pearson and Graessley<sup>9</sup> show that the proportion of dangling branched structures should increase markedly with decreasing  $R_0'$ , and in the light of the reptation concept of de Gennes<sup>10</sup> any branched structure should relax exceedingly slowly.

The minimum in  $\lambda(t)$  cannot be identified with a first state of ease  $\lambda_s'$  with any simple significance, however, since some of the untrapped entanglements will relax during the first stage of the retraction. In fact, if none of them had relaxed in the sample with  $R_0' = 0.25$ , a minimum in  $\lambda(t)$  of  $\lambda_{\min} = 1.03$  would have been reached instead of the observed value of about 1.10<sub>4</sub>.

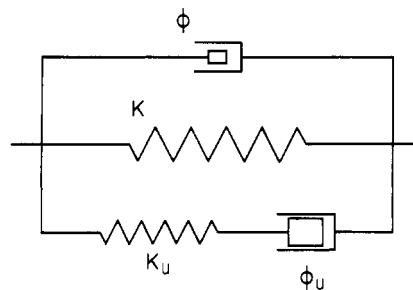


Figure 2. Mechanical model to simulate networks of cross-links and trapped entanglements together with untrapped entanglements on dangling structures.

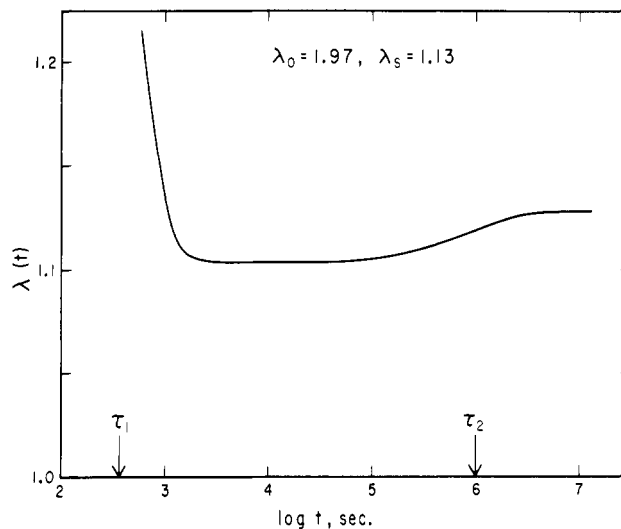


Figure 3. Retraction curve calculated for model of Figure 2 with  $C_1 = 0.864$ ,  $C_2 = -0.024$ ,  $\lambda_s = 1.128$ ,  $\tau_1 = 300$  s,  $\tau_2 = 10^6$  s.

The behavior seen in Figure 1 can be imitated qualitatively by the crude linear mechanical model shown in Figure 2. Here  $K$  is a spring constant representing the sum of the cross-link and trapped entanglement networks; if the former exerts a force proportional to  $\lambda - \lambda_0$  and the latter a force proportional to  $\lambda - 1$ , the net force is  $K(\lambda - \lambda_s)$ . The friction  $\phi$  is a measure of the retardation of the motion of these networks. The spring constant  $K_u$  refers to the contribution of the untrapped entanglements, relaxed by the dashpot  $\phi_u$  which has a much larger friction coefficient because of the branched structures. The course of retraction for this model can be expressed as  $\lambda(t) = C_1 e^{-t/\tau_1} + C_2 e^{-t/\tau_2} + \lambda_s$  where  $C_1$  and  $C_2$  can be obtained from  $\lambda_0$ ,  $\lambda_s$  and  $\lambda_{\min}$  (provided  $\tau_1$  and  $\tau_2$  are well separated);  $\tau_1$  and  $\tau_2$  are rather complicated functions of the coefficients of the model.<sup>11</sup> To compare the model with the sample with  $R_0' = 0.25$ ,  $C_1$  and  $C_2$  were calculated from  $\lambda_0$ ,  $\lambda_s$ , and  $\lambda_{\min}$ , and  $\tau_1$  and  $\tau_2$  were chosen rather arbitrarily to place the time dependence in similar regions of the time scale. The result is shown in Figure 3, which qualitatively resembles the bottom curve in Figure 1 (more extended in time scale because it was calculated for a constant temperature). No more can be expected since Hookean

elasticity has been assumed together with a single relaxation time instead of a relaxation spectrum in each of the two time scale regions. However, it shows that the essential features correspond to a model in which the contributions of trapped and untrapped entanglements are represented.

The first time constant,  $\tau_1$ , is  $3 \times 10^2$  s at 0 °C. This is nearly  $10^2$  larger than the longest relaxation time in the transition zone, corresponding to configurational rearrangement of an average strand between two entanglement loci; the latter can be estimated by applying the Rouse–Mooney theory<sup>12</sup> to viscoelastic measurements of Sanders<sup>13</sup> on a polybutadiene with 91.5% vinyl and correcting for the difference in microstructure by the free volume equation used by Rhee and Ferry,<sup>14</sup> and finally applying an experimentally determined shift factor from 25 to 0 °C. The difference may be partly due to the cyclization of vinyl groups which occurs in irradiation<sup>15</sup> and presumably stiffens the molecule as well as altering the free volume. It seems reasonable that the time scale of the first stage of the retraction is set by configurational rearrangements of strands between entanglements, whether trapped or untrapped (for low  $R_0'$ , the cross-links are greatly outnumbered). The second time constant,  $10^6$  s, is reasonable compared with the very slow relaxation times observed in lightly cross-linked conventional networks and attributed to untrapped entanglements of branched structures.

Another 1,2-polybutadiene with 88% vinyl, number-average molecular weight 236 000,  $T_g$  –18 °C (polymer B<sup>3</sup>), was studied similarly over a range of  $R_0'$  from 0.013 to 0.200. The retraction curves were similar in shape to the bottom curve in Figure 1, but with no reversal. The retraction at 0 °C was more rapid than that of polymer C at similar  $R_0'$ , because of the lower  $T_g$ , but the rate diminished rapidly with decreasing  $R_0'$ . Because of the higher molecular weight, a lower  $\nu_x$  is required to correspond to a given  $\gamma$  which determines  $T_e$ , upon which in turn the presence of dangling branched structures depends. But a small  $\nu_x$  means a small  $R_0'$  and  $\lambda_s$  is only slightly larger than 1, so a minimum below  $\lambda_s$  would be difficult to detect.

The result of relaxation of untrapped entanglements is somewhat analogous to that of a sequence of operations discussed by Flory,<sup>16</sup> in which two stages of chemical cross-links are introduced, first in the unstrained state and then in a state of strain, and some of the first-stage cross-links are subsequently removed. The predictions of Flory for  $\lambda_s$  under these circumstances (corresponding to neo-Hookean stress-strain relations) have been numerically evaluated for some specific cases.<sup>5</sup> Comparison with the bottom curve of Figure 1 is not successful, however; given the known total concentration of entanglements, the correct  $\lambda_s$  is predicted by the Flory theory only for much larger values of  $\nu_N$  and  $\nu_x$  than are actually found. The discrepancy probably arises from the assumption in the theory that the initial molecular weight is infinite; i.e., molecular ends are not taken into account.

**Acknowledgment.** This work was supported in part by the National Science Foundation, Grant No. DMR 76-09196, Polymers Program. We are indebted to Professor J. E. Willard for use of a <sup>60</sup>Co source for irradiation.

## References and Notes

- O. Kramer, R. L. Carpenter, V. Ty, and J. D. Ferry, *Macromolecules*, **7**, 79 (1974).
- R. L. Carpenter, O. Kramer, and J. D. Ferry, *Macromolecules*, **10**, 117 (1977).
- R. L. Carpenter, H.-C. Kan, and J. D. Ferry, *Polym. Eng. Sci.*, in press.
- N. R. Langley, *Macromolecules*, **1**, 348 (1968).
- J. D. Ferry, *Prelim. Rep., ARPA Mater. Summer Conf.*, **1**, 327 (1971).
- O. Kramer, V. Ty, and J. D. Ferry, *Proc. Natl. Acad. Sci. U.S.A.*, **69**, 2216 (1972).
- N. R. Langley and J. D. Ferry, *Macromolecules*, **1**, 353 (1968).
- J. D. Ferry, "Viscoelastic Properties of Polymers", 2nd ed, Wiley, New York, N.Y., 1970 Chapter 14.
- D. S. Pearson and W. W. Graessley, *Macromolecules*, **11**, 528 (1978).
- P. G. de Gennes, *J. Phys. Chem. Solids*, **36**, 1199 (1975).
- H.-C. Kan, Ph.D. Thesis, University of Wisconsin, 1979.
- Reference 8, p 259.
- J. F. Sanders, J. D. Ferry, and R. H. Valentine, *J. Polym. Sci., Part A-2*, **6**, 967 (1968).
- C. K. Rhee and J. D. Ferry, *J. Appl. Polym. Sci.*, **21**, 467 (1977).
- A. von Raven and H. Heusinger, *J. Polym. Sci., Polym. Chem. Ed.*, **12**, 2255 (1974).
- P. J. Flory, *Trans. Faraday Soc.*, **56**, 722 (1960).

## Determination of Radiation Damage in Isotactic Poly(methyl methacrylate) by X-ray Diffraction

R. P. KUSY\* and A. R. GREENBERG

Dental Research Center, University of North Carolina, Chapel Hill, North Carolina 27514. Received May 30, 1978

When a polymer is exposed to ionizing radiation, both chemical and physical changes occur. Previously chemical changes have been monitored via quantitative gas analyses,<sup>1</sup> sol–gel partition,<sup>2</sup> free-radical scavenging techniques,<sup>3</sup> or intrinsic viscosity determinations,<sup>4,5</sup> while the total damage has been measured by cryoscopy.<sup>6,8</sup> This note presents X-ray diffraction data on semicrystalline isotactic poly(methyl methacrylate) (PMMA) that verify the magnitude of radiation damage observed previously by the melting point depression technique.<sup>7,8</sup> On the assumption that the probability of radiation-induced changes are equivalent in both crystalline ( $x_c$ ) and amorphous fractions, a value for  $G(-\text{units}) \approx 15$  results from the relative decrease in crystallinity as a function of dose.

Two batches (A and B) of amorphous stereoregular PMMA were crystallized from 4-heptanone and outgassed under vacuum.<sup>9,10</sup> Additionally batch B, which had been heat treated for 2.5 h at 120 °C, was subdivided and heated for 48 h at 100 °C (designated batch B-1). All powders were irradiated *in air* at 30 °C using a Cs-137  $\gamma$ -ray source at a dose rate of 0.80 Mrad/h. Crystallinity of all powders was measured with a Philips Norelco diffractometer in the reflection mode with stabilized Cu K $\alpha$  radiation at 35 kV and 20 mA. As reported earlier,<sup>8</sup> several precautions were taken to insure an invariant baseline over the range,  $2\theta = 5$ –25°. All data were analyzed by a modified method of Hermans and Weidinger<sup>11,12</sup> whereby a correction was employed for any shifts that might occur to the amorphous halo as a function of dose.<sup>13</sup>

Table I summarizes the results of the present experiments. As was done on isotactic PMMA previously,<sup>8</sup> the heights of three crystalline reflections were scaled off the X-ray scans:  $2\theta = 8.8$ , 14.5, and 17.2°. Rather than analyzing these peaks individually, however, they were summed since a more reliable data base resulted by accumulating the crystalline ( $I_c$ ) and amorphous ( $I_a$ ) intensities on a per scan basis. Results of the regression of  $I_c$  on  $I_a$  are illustrated in Figure 1. From the intercept, which represents  $x_c = 1.0$  ( $\sum I_c = 302$ ; cf. Table II), the  $x_c$  of each sample was determined, the maximum of which equalled 0.69 (cf. Table I). When  $x_c$  was plotted against dose ( $D$ ) for each batch (Figure 2), three regression lines resulted having slopes of  $-1.09 \times 10^{-3}$ ,  $-3.16 \times 10^{-4}$ , and